

**Enhanced superradiance of quantum sources near nanoscaled media**

A. Sivan\* and M. Orenstein

*Faculty of Electrical Engineering, Technion–Israel Institute of Technology, Haifa 32000, Israel*

(Received 12 October 2018; published 26 March 2019)

We develop a rigorous theory for nanophotonic cooperative spontaneous emission of an ensemble of quantum emitters near matter, which also incorporates absorption. Such theory is highly requested since one should expect that in the field of nanophotonics the close-by emitters will emit cooperatively simultaneously with strong interaction with the exotic metamaterial complex dielectric function. The closed-form model developed here considers the buildup both of interemitter correlation over time through emitter transitions via the mutual field and of geometry-induced spatial correlation. The presence of matter alters the local density of states (LDOS), resulting in modified decay rate and emission intensity for the entire ensemble relative to values of spontaneous emission in free space. The superradiant total emission is separable into a quantum-mechanical time-dependent part and a classical space-dependent part, both being functions of the LDOS. Two distinct radiative emitter–far-field coupling mechanisms, which together account for the superradiant emission, are obtained—the coupling of every individual emitter with the far field and the coupling of emitter pairs to the far field. The calculations for superradiating emitters near silver and near-zero epsilon (NZE) materials were performed with the following results: the silver sphere augments the superradiant far-field intensity and rate by up to 400 and 1000%, respectively, while the NZE sphere enhances the far-field intensity and rate of the superradiance by approximately 1400 and 400%, respectively.

DOI: [10.1103/PhysRevB.99.115436](https://doi.org/10.1103/PhysRevB.99.115436)**I. INTRODUCTION**

The area of nanoplasmonics is a field that has undergone a substantial advancement in recent years, following the development of theoretical concepts with far-reaching applications in many applied fields of knowledge including communications, energy, and biomedicine. One central concept paramount to the realization of this area is that of the controlled emission and absorption of visible and infrared light from and to quantum structures on the nanometric scale. A fine manipulation of the emissions and absorptions of light in volumes much smaller than the characteristic dimensions of light itself will enable the manufacturing and enhancement of optical sources, optical antennas, photovoltaic cells, and many more photonic devices. Such manipulation requires control over the coupling of visible or IR photons to a more localized manifestation of energy in adequate frequencies.

One possible physical mechanism that has been at the center of intensive research over the past years is the coupling of the photons to a collective localized movement of electrons on the surface of a conducting material, conveniently named “surface plasmons.” This coupling essentially enables the photons which are characterized by a volume of  $\sim\lambda^3$ , with  $\lambda$  being the wavelength of the photon, to effectively exchange energy with electrons confined to a much smaller volume unlimited by the diffraction of light by converting a portion of the energy stored in the photons as electromagnetic fields into kinetic energy of the collection of free electrons in the

material. This conversion into electron kinetic energy in a nonideal material inevitably introduces a substantial decay due to resistive mechanisms, which seems to render this coupling less viable for practical purposes [1].

However, as it turns out, some effects predicted by quantum electrodynamics (QED), and more specifically cavity QED, could be employed to overcome this limitation. It was first proposed in the 1940’s by Purcell [2] that the rate and the amplitude of a spontaneously emitting source can be altered by changing the environment in which the source is situated, as this environment governs the number of allowed modes into which photons can be emitted. Consequently, the environment alters the probabilities of modes of photons to occupy some volume in space, which directly affects their rates of spontaneous emission. Engineering of materials to tailor the local density of states (LDOS) in order to enhance or suppress spontaneous emission rates in optical devices has been the topic of recent research [3,4].

A different effect that was studied by Dicke [5] suggests that when many identical sources are located close to one another with respect to the wavelengths of their emitted photons they interact with each other through the local photonic field so that every source affects the rates of emission of the others. As was shown in Dicke’s works, this results in a collective spontaneous emission which is characterized by a very intense and very fast emission, in comparison to what would have been observed had each source radiated independently of the others. This collective phenomenon, known as “superradiance,” essentially results in radiation intensity that peaks at  $I \propto N^2$  for  $N$  spontaneously decaying emitters rather than the classical  $I \propto N$  for independent emitters, over a time period  $N$  times shorter.

\*amirsivan89@gmail.com

Harnessing the superradiance phenomenon, along with Purcell's effect, could in theory overcome inherent losses in the photon-plasmon coupling and facilitate the realization of photonic devices in the deep subwavelength. In this paper we shall investigate the behavior of many emitters coupled to one another in the presence of exotic dielectric nanostructures, including material loss, and analyze the effect of matter mediating on multiple quantum photon sources.

While earlier work analyzing cooperative emission near a plasmonic nanoparticle incorporated a semiclassical description of the sources and emission process [6], we focus our paper on a fully quantum-mechanical system as we aim to analyze the effect of matter on the cascaded state transitions of an excited ensemble of emitters. We will investigate the behavior of a system composed of multiple quantum emitters, each described as a two-level system (TLS), set symmetrically around spherical nanoparticles of varying materials and sizes. We will focus on metallic silver and near-zero epsilon (NZE) metamaterial spheres, but the model developed here will hold to any material described by a macroscopic dielectric function. Additionally, the treatment of the system will be fully quantum mechanical. It is worth noting that the collective spontaneous emission phenomenon was extensively studied in the past several decades by many authors [7–10]. As it turns out, the term “superradiance” may refer to several closely related phenomena, some of which may be also treated classically, that differ mainly in the assumed form of excitation and representation of the sources. In the literature, there is in general some ambiguity as to the exact nomenclature and definition for these different phenomena, and thus it is important to note that in this paper we will refer the term “superradiance” to the phenomenon of collective spontaneous emission of a completely excited, but not initially correlated, sample of quantum emitters expressed in the Dicke basis.

The paper is organized as follows. Section II introduces the theoretical background necessary for the construction of our quantum description of the system. In Sec. III, the theoretical foundation of quantum mechanics in the presence of losses is reviewed. From that, the dynamics of the system are developed, and we obtain the expression for the total radiated energy. Section IV presents our calculation results for silver and NZE spheres, and discussion thereon. Final remarks and conclusions are presented in Sec. V.

## II. THEORETICAL BACKGROUND

### QED in the presence of lossy media

Consider a system consisting of multiple two-level emitters embedded in a lossless dielectric, near a lossy nanostructure. The concept of material losses, as appears in classical mechanics, is strange to the quantum-mechanical approach. Dissipation of energy in classical mechanics is employed by unidirectional conversion of energy from one form to another—usually heat, that is irreversible, and one is not faced with any mathematical or conceptual problems when one employs it. However, when approaching the problem from a quantum-mechanical point of view it is no longer possible to simply “lose” energy to some statistical irreversible mechanism; the quantum-mechanical system has to be described as a

closed system, wherein energy quanta can be transferred from one object to another according to specific “rules.”

To incorporate losses into this quantum-mechanical description, we adopt in this paper the Huttner-Barnett quantization scheme [11]. The entire space is thus described by three distinct kinds of quantum harmonic oscillators: The first describes photons as in a free-space radiation field; the second describes the bulk—a continuum of degrees of freedom, acting as a coupled reservoir that acts as an object into which the energy quanta flow; and the third is a  $N$  harmonic oscillator field describing the medium's polarization. The photonic and the polarization fields are coupled to one another. Additionally, these polarization oscillators are coupled to the reservoir, in a manner such that energy quanta may flow from them into the bulk, but not the other way around. In this way, the effect of absorption in the material is achieved.

In a system consisting of radiation, matter (which can be further decomposed to the medium polarization and the reservoir), and the interactions between them, we follow the derivation of Refs. [11–15] and others in defining the Hamiltonian of the system as

$$\hat{H} = \int d^3\mathbf{k} \int d\omega \hbar\omega \hat{\mathbf{C}}^\dagger(\omega, \mathbf{k}) \hat{\mathbf{C}}(\omega, \mathbf{k}). \quad (1)$$

The vector field operators  $\hat{\mathbf{C}}(\omega, \mathbf{k})$  account for the bulk, polarization, and vacuum radiation fields of frequency  $\omega$  and wave vector  $\mathbf{k}$  combined, and are de facto the creation and annihilation operators for an “effective vacuum,” also referred to as the “environment” throughout this paper, describing the entire space. These operators satisfy the commutation relations

$$[\hat{\mathbf{C}}(\omega, \mathbf{k}), \hat{\mathbf{C}}^\dagger(\omega', \mathbf{k}')] = \delta(\omega - \omega')\delta(\mathbf{k} - \mathbf{k}'), \quad (2)$$

with  $\delta$  being Dirac's delta distribution. Defining the spatial Fourier transform of  $\hat{\mathbf{C}}(\omega, \mathbf{k})$ ,

$$\hat{\mathbf{f}}(\mathbf{r}, \omega) = \frac{1}{(2\pi)^{3/2}} \int_{-\infty}^{\infty} d^3\mathbf{k} \sum_{\lambda=1}^2 \mathbf{e}_\lambda(\mathbf{k}) \hat{\mathbf{C}}^\lambda(\mathbf{k}, \omega) e^{i\mathbf{k}\cdot\mathbf{r}} \quad (3)$$

where  $\mathbf{e}_\lambda$  are the polarization unit vectors and  $\hat{\mathbf{f}}(\mathbf{r}, \omega)$  satisfy

$$[\hat{\mathbf{f}}(\mathbf{r}, \omega), \hat{\mathbf{f}}^\dagger(\mathbf{r}', \omega')] = \delta(\mathbf{r} - \mathbf{r}')\delta(\omega - \omega'), \quad (4)$$

we can write the inhomogeneous wave equation for the electric field [16]:

$$\begin{aligned} \nabla \times \nabla \times \hat{\mathbf{E}}(\mathbf{r}, \omega) - \frac{\omega^2}{c^2} \varepsilon(\omega) \hat{\mathbf{E}}(\mathbf{r}, \omega) \\ = i \frac{\omega^2}{c^2} \sqrt{\frac{\hbar}{\pi \varepsilon_0}} \text{Im}[\varepsilon(\omega)] \hat{\mathbf{f}}(\mathbf{r}, \omega). \end{aligned} \quad (5)$$

Here  $\varepsilon_0$  is the vacuum permittivity and  $\varepsilon(\omega)$  is the dielectric function of the material,  $c$  is the speed of light in vacuum,  $\hbar$  is the reduced Planck constant, and  $\omega$  is the angular frequency. The operator  $\hat{\mathbf{f}}(\mathbf{r}, \omega)$  acts as the stochastic noise source term, as per the dissipation fluctuation theorem [17]. To obtain a closed-form expression for the electric-field operator from this differential equation, we will use the definition of the Green's

function for the wave equation:

$$\begin{aligned} \nabla \times \nabla \times \mathbf{G}(\mathbf{r}, \mathbf{r}', \omega) - \frac{\omega^2}{c^2} \varepsilon(\mathbf{r}, \omega) \mathbf{G}(\mathbf{r}, \mathbf{r}', \omega) \\ = \mathbf{I} \delta(\mathbf{r} - \mathbf{r}'). \end{aligned} \quad (6)$$

By multiplication of the Green's function (6) by  $i(\omega^2 \hbar / c^2 \pi \varepsilon_0) \sqrt{\text{Im}[\varepsilon(\omega)]} \hat{\mathbf{f}}(\mathbf{r}, \omega)$  and by integration over the entire space, one obtains

$$\begin{aligned} \hat{\mathbf{E}}(\mathbf{r}, \omega) = i \sqrt{\frac{\hbar}{\pi \varepsilon_0}} \frac{\omega^2}{c^2} \int d^3 \mathbf{r}' \sqrt{\text{Im}[\varepsilon(\mathbf{r}', \omega)]} \\ \times \mathbf{G}(\mathbf{r}, \mathbf{r}', \omega) \hat{\mathbf{f}}(\mathbf{r}', \omega). \end{aligned} \quad (7)$$

This vector operator depends on macroscopic electromagnetic properties of the material through the imaginary part of its dielectric function, as well as on the geometry of the medium through the Green's dyadic. The environment operator  $\hat{\mathbf{f}}(\mathbf{r}, \omega)$  is the dynamical variable that will dictate the evolution of the electric field. From (4), it is clear that  $\hat{\mathbf{E}}(\mathbf{r}, \omega)$  obeys time-independent commutation relations and thus this quantization scheme is consistent. Moreover, this result is consistent with the dissipation-fluctuation theorem, as

$$\langle 0 | \hat{\mathbf{E}}(\mathbf{r}, \omega) \hat{\mathbf{E}}^\dagger(\mathbf{r}', \omega') | 0 \rangle = \frac{\hbar}{\pi \varepsilon_0} \frac{\omega^2}{c^2} \text{Im}[\mathbf{G}(\mathbf{r}, \mathbf{r}', \omega)] \delta(\omega - \omega'). \quad (8)$$

Note that for  $\mathbf{r} = \mathbf{r}'$  and under integration along the positive  $\omega$  axis (8) is a restatement of Fermi's "golden rule." In other words, the quantized electric-field operator is directly related to the LDOS, which is proportional to the decay rate of quantum systems in a given environment, and so one should be able to formulate the entire dynamics of a decaying quantum system in a general medium from knowledge of only the electric field.

### III. DYNAMICS OF THE SYSTEM

#### A. The total Hamiltonian

Having developed a theory for the Hamiltonian operator governing the radiation and material absorption in Sec. II, we now proceed to construct the Hamiltonian operator of a system containing  $N$  identical TLSs acting as emitters in the vicinity of absorbing material. Throughout this paper, the TLSs are described as dipoles.

Define the total Hamiltonian:

$$\hat{H}_{\text{tot}} = \hat{H}_F + \hat{H}_Q + \hat{H}_{QF}. \quad (9)$$

Here  $\hat{H}_F$ ,  $\hat{H}_Q$ , and  $\hat{H}_{QF}$  are the energy operators for the environment, the emitters, and the emitter-field interaction, respectively. The environment operator is composed of the "effective vacuum" vector operators developed in Sec. II,

$$\hat{H}_F = \int d^3 \mathbf{r} \int_0^\infty d\omega \hbar \omega \hat{\mathbf{f}}^\dagger(\mathbf{r}, \omega) \hat{\mathbf{f}}(\mathbf{r}, \omega), \quad (10)$$

to which we add  $N$  identical emitters, each characterized by a dipole vector  $\mathbf{d}$  and an energy gap  $\hbar \omega_Q$ . Here the collection of emitters is approximated as independent dipoles, whereas in the Dicke model the constraint on the sample to be much

smaller than the emitted wavelength resulted in all dipoles of moment strength  $d$  behaving as a single dipole of moment strength  $Nd$ . The emitter part of the Hamiltonian is simply

$$\hat{H}_Q = \frac{1}{2} \sum_{i=1}^N \hbar \omega_Q (|e\rangle_i \langle e|_i - |g\rangle_i \langle g|_i) = \frac{1}{2} \sum_{i=1}^N \hbar \omega_Q \hat{\sigma}_i^z, \quad (11)$$

where  $|e\rangle_i$  and  $|g\rangle_i$  stand for the excited and ground states of the TLS, respectively, for the  $i$ th emitter and  $\hat{\sigma}_i^z$  is Pauli's  $z$  matrix for the  $i$ th emitter.

For the interaction part, we generalize the derivation of Ref. [12] for the case of any number of emitters. The calculation is given in the Appendix, throughout which we make the rotating wave approximation (RWA) for the emitter-environment system, thereby considering only near-resonant and weak emitter-field interaction. The resulting interaction Hamiltonian is

$$\hat{H}_{QF} = - \sum_{i=1}^N \mathbf{d}_i [\sigma_i^\dagger \hat{\mathcal{E}}^{(+)}(\mathbf{r}_{Q,i}) + \sigma_i \hat{\mathcal{E}}^{(-)}(\mathbf{r}_{Q,i})], \quad (12)$$

where  $\mathbf{r}_{Q,i}$  is the position of the  $i$ th emitter, approximated as a point dipole,  $\sigma_i$  and  $\sigma_i^\dagger$  are Pauli's matrices for the  $i$ th emitter, and the vector field operators  $\hat{\mathcal{E}}^{(+)}(\mathbf{r})$  and  $\hat{\mathcal{E}}^{(-)}(\mathbf{r})$  are defined in the Appendix. Lastly, we note that an interaction term of the form  $\mathbf{d} \cdot \mathcal{E}$  contains in principle all electromagnetic interactions involving the emitters [8]; in the dipole approximation considered here for the TLS, these include Coulomb and dipole-dipole interactions.

Substituting (10)–(12) in (9) results in the expression for the total Hamiltonian of the combined environment-emitters system:

$$\begin{aligned} \hat{H}_{\text{tot}} = \int d^3 \mathbf{r} \int_0^\infty d\omega \hbar \omega \hat{\mathbf{f}}^\dagger(\mathbf{r}, \omega) \hat{\mathbf{f}}(\mathbf{r}, \omega) \\ - \frac{1}{2} \sum_{i=1}^N \hbar \omega_Q \hat{\sigma}_i^z - \sum_{i=1}^N \mathbf{d}_i [\sigma_i^\dagger \hat{\mathcal{E}}^{(+)}(\mathbf{r}_{Q,i}) + \text{H.c.}]. \end{aligned} \quad (13)$$

This Hamiltonian describes  $N$  quantum emitters in an environment that includes absorptive material, and accounts for all electromagnetic interactions of the emitters. Internal decay mechanisms of the emitters are omitted from this paper. This is appropriate when the emitters have long internal decay times, such as atoms or quantum dots which have characteristic internal decay times in the order of microseconds to milliseconds, compared to decay times of native spontaneous emission which are in the order of nanoseconds (for example, see Refs. [18,19]). As we will show in Sec. IV, this assumption is even more justified for the case of superradiance, which is characteristically a much faster process than independent spontaneous emission.

#### B. The master equation

We now develop the rate equations for the many-emitter system. The first part of this section follows literature [8,9] in the development of the general framework for the evolution of many TLSs in a radiation field, and in the second part the Hamiltonian we have developed in the previous section

is incorporated and the specific system which is the focus of this paper is considered.

Denote the density operator of the combined emitter-environment system  $\hat{\Theta}_{Q+F}(t)$ . By definition of the partial trace operation, the reduced state density operators for the quantum emitters and field are, respectively,

$$\hat{\Theta}_Q = \text{Tr}_F[\hat{\Theta}_{Q+F}], \quad \hat{\Theta}_F = \text{Tr}_Q[\hat{\Theta}_{Q+F}]. \quad (14)$$

This operator should satisfy the Schrödinger equation

$$\dot{\hat{\Theta}}_{Q+F}(t) = -i[\hat{H}, \hat{\Theta}_{Q+F}(t)] \equiv -i\hat{L}\hat{\Theta}_{Q+F}(t), \quad (15)$$

where  $\hat{L}$  is the Liouville operator  $\hat{L}\hat{X} = [\hat{H}, \hat{X}]$  and  $\hat{H}$  is the system's total Hamiltonian (13). We assume that in the initial state there are no emitted photons and denote the start condition for the field part as  $\hat{\Theta}_F(0) = |\{0\}\rangle\langle\{0\}|$ . Since there is no radiation at time  $t = 0$ , the density matrix operator is separable at that instant, so that

$$\hat{\Theta}_{Q+F}(0) = \hat{\Theta}_Q(0)\hat{\Theta}_F(0) = \hat{\Theta}_Q(0) \otimes |\{0\}\rangle\langle\{0\}|. \quad (16)$$

Solving (15) [cf. (16)] for  $\hat{\Theta}_Q$ , we assume that the emitter-field correlation time is negligibly short in comparison to the characteristic time scale of the system's evolution since, as pointed out before, the coupling of the field to the emitters is considered weak and near resonance, and the characteristic size of the sample is assumed to be smaller than the emitted wavelength. In these conditions we can apply the Born-Markov approximation. We obtain a system of ordinary differential equations

$$\begin{aligned} \dot{\hat{\Theta}}_Q(t) = & -i\omega_Q \sum_i [\hat{\sigma}_i^z, \hat{\Theta}_Q(t)] \\ & - \sum_{i,j} \{A_{ij}^+ [\hat{\sigma}_i^\dagger, \hat{\sigma}_j \hat{\Theta}_Q(t)] \\ & - A_{ij}^- [\hat{\sigma}_j, \hat{\Theta}_Q(t) \hat{\sigma}_i^\dagger]\}, \end{aligned} \quad (17)$$

with the definition  $A_{ij}^\pm = (\Gamma_{ij} \pm i\delta\omega_{ij})/2$ , where

$$\Gamma_{ij} = \frac{2\omega_Q^2 d^\mu d^\nu}{c^2 \hbar \epsilon_0} \text{Im}[\mathbf{G}_{\mu\nu}(\mathbf{r}_{Q,i}, \mathbf{r}_{Q,j}, \omega_Q)] \quad (18)$$

and

$$\delta\omega_{ij} = \frac{2d^\mu d^\nu}{\pi \hbar \epsilon_0} PV \int_0^\infty d\omega \frac{\omega^2}{c^2} \frac{\text{Im}[\mathbf{G}_{\mu\nu}(\mathbf{r}_{Q,i}, \mathbf{r}_{Q,j}, \omega_Q)]}{\omega - \omega_Q} \quad (19)$$

are the real valued real and imaginary parts of  $A_{ij}^\pm$ , respectively. In (17) and in the following, unless otherwise specified, the sums run from 1 to  $N$  for each index specified under the summation symbol. The Greek letter subscripts and superscripts for the vectors and tensors are summed together over all spatial coordinates.

The real part of  $A_{ij}^\pm$ , given in (18), corresponds to the radiative decay rate change of the emitter located at  $\mathbf{r}_{Q,i}$ , due to its coupling through the radiation field to the emitter in  $\mathbf{r}_{Q,j}$ . Note that  $\Gamma_{ij}$  encapsulates two distinct phenomena: When  $i = j$ , one simply obtains Einstein's A coefficient for the  $i$ th emitter, describing its interaction with the field; however, the terms with  $i \neq j$  describe a second radiative coupling mechanism

between the sample and the field, through interactions of pairs of emitters with the field.

The imaginary term of  $A_{ij}^\pm$  corresponds to the nonradiative (virtual) transitions of energy between the emitters in  $\mathbf{r}_{Q,i}$  and  $\mathbf{r}_{Q,j}$ . Just as for the radiative term,  $\delta\omega_{ij}$  also describes two different phenomena: When  $i = j$ ,  $\delta\omega_{ij}$  is equal to the Lamb shift of the  $i$ th emitter, while  $i \neq j$  describes dipole-dipole interactions between the  $i$ th and  $j$ th emitters. These shifts, although divergent, are cut off at frequencies corresponding to the size of the sample [20], resulting in a negligible effect on the superradiant process [21]. For now, for the sake of completeness, we shall not omit  $\delta\omega_{ij}$ . Substituting (18) in (17) and transforming back to the Schrödinger picture yields

$$\begin{aligned} \dot{\hat{\Theta}}_Q(t) = & -i\omega_Q \sum_i [\hat{\sigma}_i^z, \hat{\Theta}_Q(t)] \\ & - \sum_{i,j} \left\{ \frac{\Gamma_{ij}}{2} [\hat{\sigma}_i^\dagger \hat{\sigma}_j \hat{\Theta}_Q(t) + \hat{\Theta}_Q(t) \hat{\sigma}_i^\dagger \hat{\sigma}_j - 2\hat{\sigma}_j \hat{\Theta}_Q(t) \hat{\sigma}_i^\dagger] \right. \\ & \left. + \frac{i\delta\omega_{ij}}{2} [\hat{\sigma}_i^\dagger \hat{\sigma}_j, \hat{\Theta}_Q(t)] \right\}. \end{aligned} \quad (20)$$

This expression is the master equation of the emitters sample. Its solution governs the evolution of the emitters in time, from which the temporal behavior of the emitted electromagnetic field can be derived.

A system of  $N$  emitters can be fully described by a density matrix of dimension  $2^N$ , which is the dimension of the Hilbert space spanned by  $N$  two-level systems. Calculation of a general setting of emitters might prove to be impractical, as we are required to solve those coupled ordinary differential equations (ODEs) (e.g.,  $1024 \times 1024$  coupled ODEs for only ten emitters). Therefore, we shall deal with systems in which all the emitters are indistinguishable—such that the states are symmetrical. In practice, this indistinguishability means that every emitter will experience the exact same environment as the others. That means that if one had put serial numbers on the emitters an observer situated on any emitter would not have been able to tell on which emitter he was situated based on any physical measurement that he could perform, so that the dynamics of the problem are invariant to the indices of the emitters. That also imposes restrictions on the generality of the geometrical setting of the problem, and so the model presented in this paper will be valid only for settings with axial symmetry. Specifically, in this paper we examine a system composed of a spherical nanoparticle having quantum emitters located equidistantly from it on a ring around its equator—however, many more symmetrical settings are viable.

It is well known that the problem of  $N$  TLSs is isomorphic to the problem of  $N$  spinors with spin  $1/2$ . Thus, three quantum numbers can fully span the  $2^N$ -dimensional Hilbert space— $|j, m, \lambda\rangle$ , where  $0 \leq j \leq N/2$  is the cooperation number,  $-j \leq m \leq j$  is the total excitation, and  $\lambda$  is the degeneracy of the  $(j, m)$  state. In dealing only with indistinguishable emitters in a symmetrical state, which are initially fully excited, it can be shown (e.g., in Ref. [9]) that the only quantum number relevant to the evolution of the system is  $|m| \leq j = N/2$ , and so it is clearly sufficient to work in a subspace of dimension  $N + 1$ .

We replace ladder operators  $\hat{\sigma}_i$  of the individual emitters with collective ladder operators for symmetrical states defined by

$$\begin{aligned}\hat{\Sigma}|j, m\rangle &= \sqrt{j(j+1) - m(m-1)}|j, m-1\rangle, \\ \hat{\Sigma}^\dagger|j, m\rangle &= \sqrt{j(j+1) - m(m+1)}|j, m+1\rangle \\ \hat{\Sigma}^z|j, m\rangle &= m|j, m\rangle\end{aligned}\quad (21)$$

and rewrite the Hamiltonian:

$$\begin{aligned}\hat{H}_{\text{tot}} &= \int d^3\mathbf{r} \int_0^\infty d\omega \hbar\omega \hat{\mathbf{f}}^\dagger(\mathbf{r}, \omega) \hat{\mathbf{f}}(\mathbf{r}, \omega) - \frac{1}{2} \hbar\omega_Q \Sigma^z \\ &\quad - \frac{1}{N} \sum_i \mathbf{d}_i \{ \Sigma^\dagger \hat{\mathbf{E}}^{(+)}(\mathbf{r}_{Q,i}) + \text{H.c.} \}.\end{aligned}\quad (22)$$

The interaction part in the Hamiltonian (13) consists of a summation of multiplications of the electric-field operator at points  $\mathbf{r}_{Q,i}$  and the  $i$ th emitter operators. By replacing the individual emitter operators with the collective operators and normalizing by a factor  $N$  we in fact state that the average electrical field acts on the entire sample. Assuming that the system of emitters and material is spatially symmetrical, as it is in our case, this approximation is good.

Solving for the master equation with the new Hamiltonian, one arrives at

$$\begin{aligned}\dot{\hat{\Theta}}_Q(t) &= -i\omega_Q [\hat{\Sigma}^z, \hat{\Theta}_Q(t)] \\ &\quad - \frac{\Gamma}{2} [\hat{\Sigma}^\dagger \hat{\Sigma} \hat{\Theta}_Q(t) + \hat{\Theta}_Q(t) \hat{\Sigma}^\dagger \hat{\Sigma} - 2\hat{\Sigma} \hat{\Theta}_Q(t) \hat{\Sigma}^\dagger] \\ &\quad + i\delta\omega [\hat{\Sigma}^\dagger \hat{\Sigma}, \hat{\Theta}_Q(t)],\end{aligned}\quad (23)$$

with

$$\Gamma = \frac{1}{N^2} \sum_{i,j} \Gamma_{ij} \quad (24)$$

and

$$\delta\omega = \frac{1}{N^2} \sum_{i,j} \delta\omega_{ij} \quad (25)$$

being the averaged rate and shift factors, each containing both of their respective environment coupling and virtual interaction mechanisms. Lastly, since we consider systems wherein the entire sample is initially excited, it is straightforward to show that  $\hat{\Theta}(t)$  is diagonal and so the master equation in its final form is

$$\dot{\hat{\Theta}}_Q(t) = -\frac{\Gamma}{2} [\hat{\Sigma}^\dagger \hat{\Sigma} \hat{\Theta}_Q(t) + \hat{\Theta}_Q(t) \hat{\Sigma}^\dagger \hat{\Sigma} - 2\hat{\Sigma} \hat{\Theta}_Q(t) \hat{\Sigma}^\dagger]. \quad (26)$$

This equation describes a lossy process with no level shifts due to virtual interactions. The absence of the  $\delta\omega$  term stems, in this case, from our choice of initial conditions, and not from the negligibility of  $\delta\omega$  that was discussed above. The exact state of the emitters at any time can be extracted from this

equation. Moreover, the evolution of the expectation value of any operator  $\hat{A}$  that does not commute with the emitter operators (21) can be evaluated, using the identity  $\langle \hat{A} \rangle = \text{Tr}(\hat{A}\hat{\Theta})$ . It is clear from (26) that in the general case the temporal behavior of the system is completely different from the decay admitted by a semiclassical analysis of a collection of emitters near a nanoparticle [6].

### C. Total radiated power

In order to calculate the total power radiated from the superradiating sample, we have to evaluate the evolution of the operators describing the environment state. Since we can find the time dependence of any operator that acts on the emitters, from (26), our goal is to find the radiation intensity function of the system in terms of emitter operators. By Heisenberg's equation one obtains

$$\dot{\hat{\mathbf{f}}} = \frac{i}{\hbar} [\hat{H}, \hat{\mathbf{f}}] = \frac{i}{\hbar} [\hat{H}_F + \hat{H}_{QF}, \hat{\mathbf{f}}], \quad (27)$$

and substituting the field and interaction Hamiltonian and formally integrating yields

$$\begin{aligned}\hat{\mathbf{f}} &= \frac{1}{N} \frac{\omega^2}{c^2} \sqrt{\frac{\text{Im}[\varepsilon(\mathbf{r}, \omega)]}{\hbar\pi\varepsilon_0}} \\ &\quad \times \sum_i \mathbf{G}^*(\mathbf{r}_{Q,i}, \mathbf{r}, \omega) \mathbf{d}_i \int_0^t d\tau e^{-i\omega(t-\tau)} \hat{\Sigma}(\tau).\end{aligned}\quad (28)$$

Under the Born-Markov approximation, we may assume that  $\hat{\Sigma}(\tau)e^{-i\tau\omega_Q}$  is slowly varying so one may pull it out of the integral (28) at time  $t$  and take the upper bound of the integral to infinity [12]. Then, using (7), the expression for the electric-field operator at time  $t$  is

$$\begin{aligned}\hat{\mathbf{E}}(\mathbf{r}, \omega; t) &= i \frac{e^{-it\omega_Q} \hat{\Sigma}(t)}{N} \frac{\omega^2}{c^2} \frac{1}{\pi\varepsilon_0} \\ &\quad \times \sum_i \mathbf{d}_j \text{Im}[\mathbf{G}(\mathbf{r}, \mathbf{r}_{Q,i}, \omega)] \zeta(\omega_Q - \omega) \\ &\equiv e^{-it\omega_Q} \hat{\Sigma}(t) \Psi(\mathbf{r}, \omega).\end{aligned}\quad (29)$$

The intensity at a far-field point  $\mathbf{R}$  is related to the electric-field operator through the known relation  $I(\mathbf{R}, t) = \frac{1}{2\eta_0} \langle \hat{\mathbf{E}}^\dagger(\mathbf{R}, t) \hat{\mathbf{E}}(\mathbf{R}, t) \rangle$ . Up to a constant with respect to time, this quantity is the expectation value of the operator  $\hat{\Sigma}^\dagger \hat{\Sigma}$ , which, clearly, is an operator acting on the emitters. Therefore, its evolution is given completely from (26). Under substitution of (29) and negligence of energy shift terms, and integration of  $I(\mathbf{R}, t)$  over the surface of a sphere with radius  $R$ , one obtains the expression for the total radiated power from the system:

$$\begin{aligned}I_{\text{tot}}(t) &= \frac{1}{2\eta_0} \frac{\omega_Q^4}{\varepsilon_0^2 c^4} \langle \hat{\Sigma}^\dagger(t) \hat{\Sigma}(t) \rangle \\ &\quad \times \frac{1}{N^2} \sum_{i,j} \int d\Omega R^2 \mathbf{d}_j \mathbf{Z}_j(\omega_Q) \mathbf{Z}_i(\omega_Q) \mathbf{d}_i^T,\end{aligned}\quad (30)$$

where for brevity we have denoted the imaginary part of the Green's function  $\mathbf{Z}_i(\omega_Q) = |\text{Im}[\mathbf{G}(\mathbf{R}, \mathbf{r}_{Q,i}, \omega_Q)]|$ .

This expression is the main result of this paper. It is composed of a temporal part, which is quantum mechanical in nature and is in fact contained solely in the zero-gap correlation function of the collective emitter ladder operator, and a spatial part, which is a solution to a scattering problem with boundary conditions embodied in the Green's functions. However, the rate by which the temporal part is governed is  $\Gamma$  from expression (24), which is also dependent on the boundary conditions expressed via the Green's function. It is straightforward to verify that, in free space and with the dipole approximation conditions  $\forall i, j : |\mathbf{r}_i - \mathbf{r}_j| \ll \lambda$  and  $\mathbf{d}_i = \mathbf{d}_j$ , Dicke's superradiance is obtained.

We restate (30) as

$$I_{\text{tot}}(t) = \frac{1}{N} I_0 T(t) F(\{\mathbf{r}_Q\}), \quad (31)$$

where  $T(t) = \langle \hat{\Sigma}^\dagger(t) \hat{\Sigma}(t) \rangle$  is the zero-gap first-order correlation function of the collective ladder operators,

$$I_0 = \frac{1}{6\eta_0\pi\epsilon_0^2} \frac{\omega_Q^4}{c^4} |\mathbf{d}|^2 \quad (32)$$

is the known result for total radiated intensity of a single dipole in free space, and

$$F(\{\bar{\mathbf{r}}\}) = \frac{1}{N} \frac{3}{|\mathbf{d}|^2} \sum_{i,j} \int R^2 d\Omega \mathbf{d}_j \mathbf{Z}_j(\omega_Q) \mathbf{Z}_i(\omega_Q) \mathbf{d}_i^T \quad (33)$$

will be denoted the spatial enhancement factor of the emitter-matter system, accounting for the electromagnetic scattering from the sphere for the fields of  $N$  emitters. This term is the same one as the classical one, and thus, in contrast to the purely quantum-mechanical temporal evolution, it may be also obtained from a semiclassical analysis [6]. It encapsulates both interference and the effect the material has on the power of the scattered fields. The factor is proportional to the rate of energy radiated to the far field from several dipole emitters [22], and we have elected to normalize it such that when  $\forall i, j : |\mathbf{r}_i - \mathbf{r}_j| \gg \lambda$  it will tend to a value of 1. In the above we have applied the notation  $\{\bar{\mathbf{r}}\} = \{\mathbf{r}_{Q,1}, \mathbf{r}_{Q,2} \dots \mathbf{r}_{Q,N}\}$ .

## IV. CALCULATION RESULTS AND DISCUSSION

### A. The Green's function

We focus in this paper on indistinguishable emitters on a symmetrical setting, thus the most straightforward choice of shape for the absorptive material would be a sphere, conveniently placed at the origin. We will use the expression for the Green's function from the literature [23] in spherical coordinates:

$$\begin{aligned} \mathbf{G}(\mathbf{r}, \mathbf{r}') &= -\frac{1}{k_0^2} \hat{\mathbf{r}} \hat{\mathbf{r}} \delta(\mathbf{r} - \mathbf{r}') \\ &+ i \frac{k_0}{4\pi} \sum_{v,mn} c_{mn} [\mathbf{F}_{v,mn}^{(1)}(k_0\mathbf{r}) \mathbf{F}_{v,-mn}^{(3)}(k_0\mathbf{r}') \\ &- \alpha_{v,l}(k_0, k_1, a) \mathbf{F}_{v,mn}^{(3)}(k_0\mathbf{r}) \mathbf{F}_{v,-mn}^{(1)}(k_0\mathbf{r}')], \quad (34) \end{aligned}$$

which expresses the scattering object as a superposition of its vector spherical harmonic components  $\mathbf{F}_{v,mn}^{(s)}(k_0\mathbf{r})$  as well

as their respective material dependent reflection coefficients  $\alpha_{M,l}(k_0, k_1, a)$  and the sequence coefficients  $c_{mn}$  as defined in Ref. [23] with the indices  $v = \{M, N\}$ ,  $1 \leq n \leq K$ , and  $|m| \leq n$  for some integer  $K$ . Here,  $k_0$  and  $k_1$  are the electromagnetic field's wave numbers in free space and inside the sphere, respectively,  $a$  is the radius of the sphere,  $\mathbf{r}$  is the position of the field's source, and  $\mathbf{r}'$  is the point of measurement, with respect to the origin of axes. This expression is easily calculable numerically. In the following section, the cutoff integer was chosen to be  $K = 12$  for all cases, as for all calculations the 12th and higher elements of the sequences were found to be negligible in comparison to the convergent results.

### B. Figures of merit

As evident from Secs. II and III, description of the system of quantum emitters and matter is complex and its dynamics are suitably involved, even when considering a relatively simple case of symmetrical configuration of identical emitters. Because of this complexity, it is important to introduce definitions for some figures of merit to quantify the results. In measuring the total radiated energy from the radiating system, various authors [5,7–10] normalize the energy with respect to the total radiated energy of a single emitter in vacuum. However, because of the intricate dependence of the total radiated energy on the number of sources and the geometry of the problem, it will not always be sensible to normalize the spatial enhancement factor with respect to a single emitter in free space, where neither the geometry of the problem nor the matter is considered. In our case a reasonable figure of merit would be

$$\chi(\{\bar{\mathbf{r}}\}) = \frac{I_{\text{tot}}(\text{Matter})}{I_{\text{tot}}(\text{Vacuum})}. \quad (35)$$

Here, the expressions for the radiated power  $I_{\text{tot}}(\text{Matter})$  and  $I_{\text{tot}}(\text{Vacuum})$  are both evaluated for the same number of emitters with the same geometrical setting, in the presence and absence of the material, respectively. This figure of merit will enable us to quantify the change in the total radiated power when matter is introduced.

Similarly, the effect of the matter on the rate of superradiant emission will be evaluated through the ratio between the decay rate of interacting emitters in the presence of the material and that of independently emitting emitters in free space. We define the effective decay enhancement factor

$$\gamma = \frac{1}{N} \sum_{i,j} \Gamma_{ij} A^{-1} = N \Gamma A^{-1}, \quad (36)$$

where  $\Gamma$  is defined in (24) and  $A$  is Einstein's  $A$  coefficient. We emphasize again the importance of the geometrical symmetry of the system on the correctness of this quantity. An important remark about  $\gamma$  is that the decay rate  $\Gamma$  measures the rate at which the system of emitters decays, into both radiative and nonradiative modes. To obtain the relation between radiative and nonradiative mechanisms of energy decay, we define the radiation efficiency factor

$$\eta_R = \frac{P_{\text{rad}}}{P_{\text{abs}} + P_{\text{rad}}}, \quad (37)$$

where  $P_{\text{rad}}$  and  $P_{\text{abs}}$  are the total radiated and total absorbed powers, respectively. It is straightforward to see that  $P_{\text{rad}} \propto F(\{\bar{\mathbf{r}}\})$ . Similarly,  $P_{\text{abs}}$  is proportional to  $F(\{\bar{\mathbf{r}}\})$  but with the integral calculated from the center of the sphere to its radius, under proper alteration of the vector spherical harmonics and scattering coefficients in expressions for the Green's functions [23]. Convenient closed expressions for  $P_{\text{rad}}$  and  $P_{\text{abs}}$  can be found, for example, in Ref. [22]. Then, it is natural to alter (35) to include  $\eta_R$ , so that

$$g(\{\bar{\mathbf{r}}\}) = \eta_R \frac{I_{\text{tot}}(\text{Matter})}{I_{\text{tot}}(\text{Vacuum})}. \quad (38)$$

This quantity is called the ‘‘superradiance intensity enhancement factor,’’ and it assesses the enhancement of the total radiated power in the vicinity of material while also considering the amount of power dissipated into losses in the material.

In Sec. III we have shown that one can divide the rate coefficients (18) into spontaneous emission rates of the individual emitters and emission rates associated with pairwise interaction with the environment. Upon inspection of (33), it can be immediately seen that a similar analysis would yield the contribution of each of the coupling mechanisms to the total amount of power radiated from the system. This can be done by introducing the quantity

$$\zeta(\{\bar{\mathbf{r}}\}) = \frac{\sum_{i,j} \int R^2 d\Omega_j \mathbf{Z}_j(\omega_Q) \mathbf{Z}_i(\omega_Q) \mathbf{d}_i^T}{\sum_i \int R^2 d\Omega [\mathbf{d}_i \mathbf{Z}_i(\omega_Q)]^2}, \quad (39)$$

which is the ratio between the total radiated power of the entire sample in the presence of the material and the sum of the contributions of each emitter as if it is radiating independently from the others in the same geometrical setting, including the matter. When  $\zeta > 1$  the cross terms of the numerator corresponding to the pairwise interaction with the environment are enhancing the total radiated power, while when  $\zeta < 1$  the pairwise interaction inhibits the radiated power. The amount of enhancement or inhibition of the radiated power resulting from the interference of emitters can therefore be assessed from this figure of merit.

### C. Collective spontaneous emission in free space

Before proceeding to analyze test cases of superradiance assisted by a medium, it will be instructive to analyze several cases in free space. The derivation of the model was done under the assumption that there is absorptive material present

in the system, and indeed the electric-field vector operator is directly related to the imaginary part of the dielectric function of the material as is evident in (7). Therefore, at first glance, it is impossible to use this model in free space. However, the expression for the total radiated power (30) is independent of the material's dielectric function, and so in practice we can calculate the radiated intensity in free space by considering the Green's dyadic in vacuum. This toy model exploration will help us develop some intuition on the influence of the emitter setting on the process of superradiance, with no regard to the contributions of the material to the process. Throughout this section, we consider the emitters to be set on rings of varying radii, but always around the equator of the sphere, such that the center of the ring coincides with the center of the sphere. The emitter dipoles themselves, having to satisfy the indistinguishability condition, are all directed in the same manner relative to the sphere and the other emitters.

We now turn to investigate the collective spontaneous emission of several identical emitters, set symmetrically on rings of varying radii in free space. Figure 2 shows the radiated power of a sample of ten emitters, normalized by the radiated power of a single emitter,  $I_0$ , vs time. Each subplot shows the radiated power for each of the three principle directions, for three ring radii— $r = 0.01\lambda$ ,  $0.015\lambda$ , and  $0.02\lambda$ . The dipole moment strength for the emitters is  $|d| = 3q_e[c][\text{nm}] \approx 144[\text{D}]$ , and the emitted wavelength is  $\lambda = 600[\text{nm}]$ . The graphs match in shape those obtained for superradiance in literature (for example, in Refs. [7,8,10]), exhibiting the same characteristic delayed peak. Comparisons between the three subplots show substantial differences, spanning several orders of magnitude, for both time and radiated power. These can be explained through relatively intuitive considerations. For example, for the radial case [Fig. 1(a)] the superradiant process is the slowest and weakest. The closer the emitters are to one another, the slower and weaker the process is, as predictable if one considers the sources as classical dipoles, since identical dipoles oriented in opposing directions will tend to cancel one another. On the other hand, parallelly oriented dipoles [Fig. 1(b)] will act as one stronger source when brought closer together. Indeed, in this setting the process is stronger and faster than in the radial case by about three orders of magnitude. It is evident that in the elevational setting the process is less susceptible to the distances between emitters than in the other two cases. This is also expected if one considers that for the radial and azimuthal settings higher multipolar moments are present and contribute to the

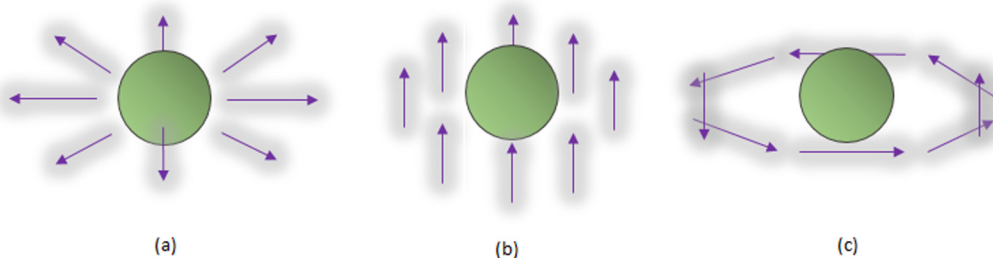


FIG. 1. Schemes of the three principle emitter orientations, for eight emitters around a nanoparticle: (a) radial ( $\hat{r}$ ) orientation, (b) elevational ( $\hat{\theta}$ ) orientation, and (c) azimuthal ( $\hat{\phi}$ ) orientation.

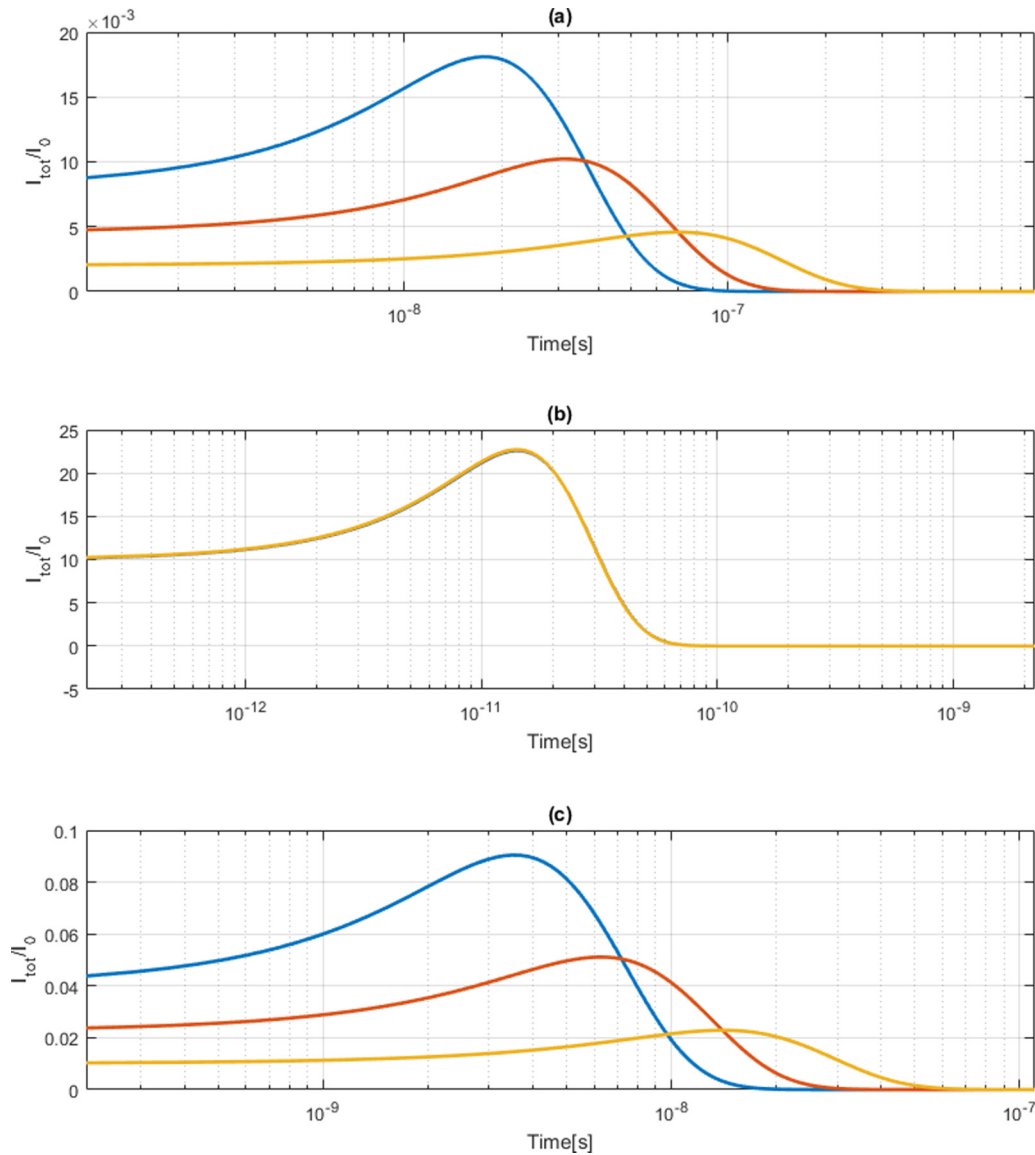


FIG. 2. Normalized total radiated power vs time for ten identical quantum emitters set equidistantly in free space on a ring of radii  $r = 0.01\lambda$  (yellow line),  $r = 0.015\lambda$  (red line), and  $r = 0.02\lambda$  (blue line). The emitters are set in (a) radial ( $\hat{r}$ ) orientation, (b) elevational ( $\hat{\theta}$ ) orientation, and (c) azimuthal ( $\hat{\phi}$ ) orientation.

total radiated intensity. These are more appreciable when the sources are farther away and negate one another less. It is important to note the significant impact that the orientations of emitters have on the results; the strengths and durations of the superradiant pulse span more than three orders of magnitude for the ten emitters considered here. For a larger number of emitters, these discrepancies will grow. Thus, it is clear that the orientations and setting of the emitters, which were largely neglected in previous analyses of collective spontaneous emission, are key determinant factors for superradiance.

The free-space analysis is also important since it confirms a crucial assumption that we have made in Sec. III. For the chosen wavelength of  $\lambda = 600$  [nm] the characteristic sample size is at most  $\sim 25$  [nm], which takes light less than one tenth of a femtosecond to traverse; this is about five orders of magnitude faster than the characteristic time scale of fastest process presented in Fig. 2. Therefore, the assumption that

retardation effects are negligible across the sample, as well as the Born-Markov approximation, central in the derivation of the model, are justified. Note, however, that for a very large number of emitters the characteristic time scale of the evolution will approach the optical cycle time, as the superradiant process time scales like  $1/N$ . Therefore, for  $N \gg 1$  these assumptions will no longer be valid [8]. However, in this paper we focus on smaller samples.

#### D. Collective spontaneous emission near a silver nanoparticle

The dielectric function for the silver is at  $\lambda = 600$  [nm], following Ref. [24]. The expression for the total radiated power (31) is separated into spatial and temporal parts, with a rate factor that also strongly depends on the spatial setting. The shape of the graph of the time-dependent radiated power will therefore be identical for any considered setting, but will be

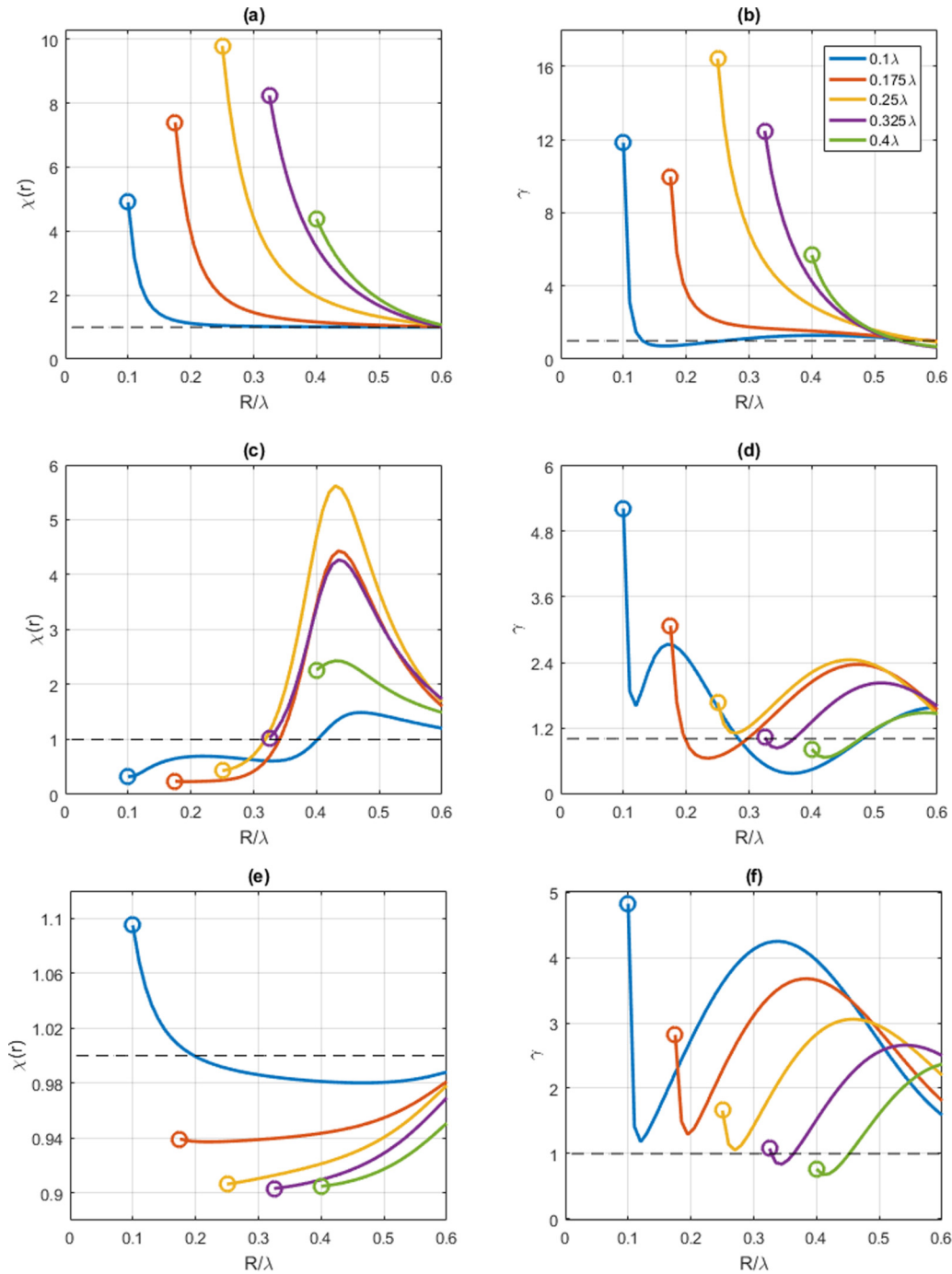


FIG. 3.  $\chi(\{\vec{r}\})$  and  $\gamma$  for ten identical emitters set equidistantly around the equators of silver spheres of varying radii (color coded) vs distance from the center of the spheres. (a, c, e)  $\chi(\{\vec{r}\})$  for radial, elevational, and azimuthal orientations, respectively. (b, d, f)  $\gamma$  for radial, elevational, and azimuthal orientations, respectively.

stretched or contracted by the factors  $F(\{\vec{r}\})$  and  $\Gamma$ , depending on the geometry of the system. Thus, we will concentrate on the influence of the geometry on these factors to assess the effect matter has on superradiance, by comparing  $\chi(\{\vec{r}\})$  and  $\gamma$  as defined in (35) and (36), respectively, for different cases. These figures of merit are presented in Fig. 3 for radial (a, b), elevational (c, d), and azimuthal (e, f) orientations of identical emitters set equidistantly around the equators of silver spheres of varying radii, at distances of  $R/\lambda$ , from the center of the spheres. Throughout the following sections, the graphs are

color coded with respect to the radii of the spheres. The circles denote the points for which  $R/\lambda = a$ —with  $a$  being the radius of the respective sphere—below which the figures of merit are not measured. For the radial orientation, it is clear from subplots (a) and (b) that the silver nanosphere enhances the LDOS, so that the emitters radiate significantly stronger and faster to the far field compared to the radial free-space case. Whereas in free space the radiated power was greatly inhibited when the emitters were pointing radially, here the sphere enhances the radiation. On the other hand, the  $\hat{\theta}$

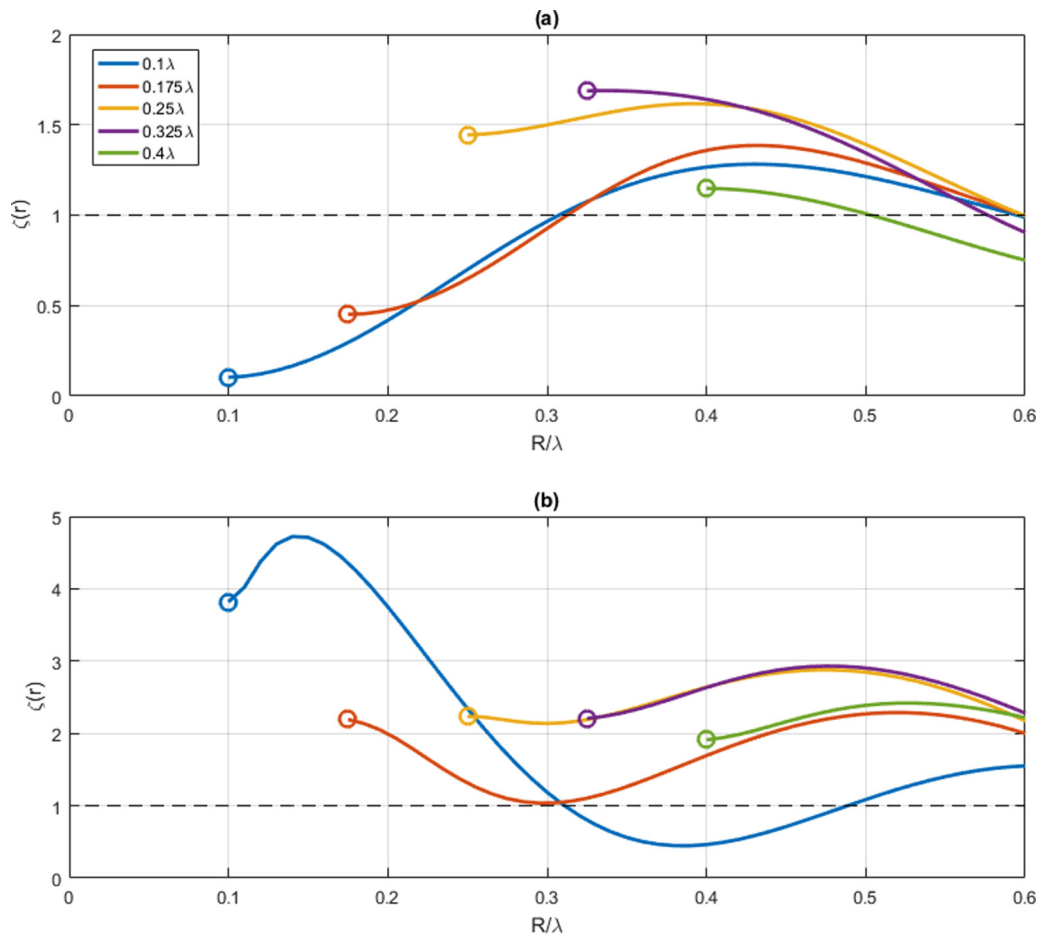


FIG. 4.  $\zeta(\{\vec{\mathbf{r}}\})$  for ten identical emitters set equidistantly around the equators of silver spheres of varying radii (color coded) vs distance from the center of the spheres. The emitters are set in (a) radial orientation and (b) elevational orientation.

oriented emitters (c, d) experience inhibition in close vicinity of the sphere in comparison to free space, and enhancement at a distance  $R \approx 0.42\lambda$  from the center of the sphere. This can again be explained through classical electromagnetism considerations, as like-oriented dipoles would induce an equal and opposite dipole moment on a metallic sphere they are adjacent to, resulting in destructive interference and weaker radiation. Note that close to the sphere the decay rate  $\gamma$  is still high, due to nonradiative losses in the absorptive silver.

Around  $R \approx 0.42\lambda$  from the center of the sphere, the phase of the induced dipole moment results in constructive interference with the sources themselves so the total radiation is enhanced. For the azimuthal orientation (e, f) the image charges on the sphere would imitate another ring of dipoles set head-to-tail with respect to one another, resulting in overall weak coupling to the far field and decay into both dissipative modes in the material and near-field modes. Since in the  $\hat{\phi}$  setting the introduction of matter further weakens a setting which did not couple strongly to the far field in the first place, we will not discuss it. Further insight into the silver sphere cases could be obtained by examining  $\zeta(\{\vec{\mathbf{r}}\})$  defined in (39) for ten emitters at different distances around silver spheres of different radii, as in Fig. 4.

As mentioned before,  $\zeta(\{\vec{\mathbf{r}}\})$  quantifies the contribution of the pairwise emitter interaction with the far field. For the  $\hat{r}$  orientation [Fig. 4(a)], it can be seen that close to the smaller

spheres where  $\zeta < 1$  it is the individual emitter interaction that mainly contributes to the coupling of the sample to the far-field modes as is expected if one considers the effect that a silver sphere has on the total far-field radiation when a classical dipole is located adjacent to it perpendicular to its surface. However, for larger spheres and farther away from their surfaces, there is a region where the pairwise interaction is in fact the main contributor of radiated power—as would be classically predictable from the analogy of dipoles inducing higher multipolar moments on the silver sphere. For the  $\hat{\theta}$  orientation, the emitter-pair interactions enhance and inhibit the coupling to the far field periodically, over period lengths of approximately  $\lambda/2$ , further reaffirming that the mutual interferences between the emitters and the silver sphere determine the total radiated power. Another aspect in the analysis of material influence on the emission is the consideration of power dissipation within the sphere. Higher rates of decay near the surfaces of silver imply that a significant portion of the power stored in the emitters is in fact transferred into absorptive modes. The figure of merit  $g(\{\vec{\mathbf{r}}\})$  defined in (38) considers power dissipation into nonradiative modes in the sphere and admits a measure of assessing the effectiveness of the introduction of matter. This is plotted in Fig. 5 for various sphere radii and orientations.

Comparing Fig. 5(a) with Fig. 3(a), it is evident that dissipative losses greatly reduce the efficiency of the radial

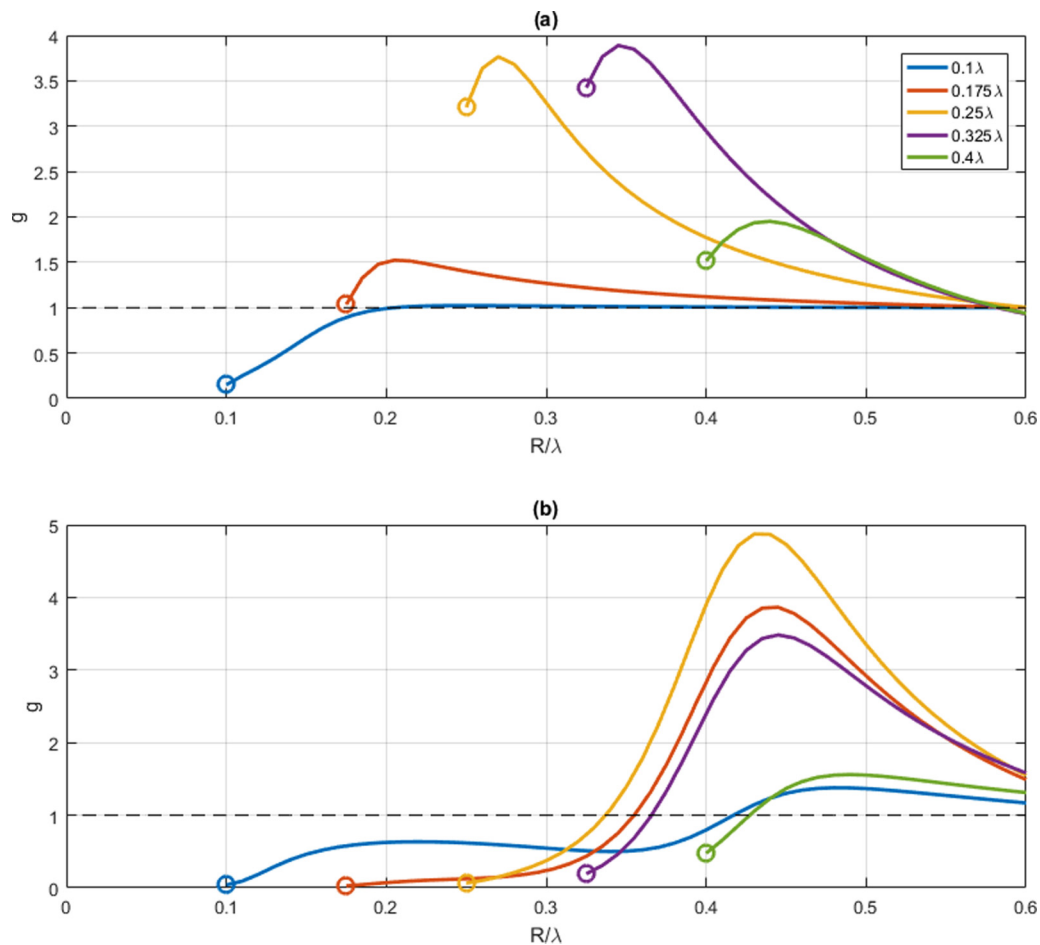


FIG. 5.  $g$  for ten identical emitters set equidistantly around the equators of silver spheres of varying radii (color coded) vs distance from the center of the spheres. The emitters are set in (a) radial orientation and (b) elevational orientation.

setting. The highest enhancement occurs at distances of about  $0.05\lambda$  from the surface of the spheres, where the dissipation due to absorptive losses is less dominant and the suppression of multipolar constructive induction on the sphere is concurrently minimal. Similar comparison for the elevational setting admits that for the  $\hat{\theta}$  case radiation is more efficient around the  $R \approx 0.42\lambda$  point from the center of the sphere. It can be then deduced that introduction of silver nanospheres to both  $\hat{r}$ - and  $\hat{\theta}$ -directed emitters at a certain range of distances will result in a stronger and faster superradiance, in comparison to systems where matter is absent. It is important to note, however, that for the radial case the total superradiated power will still be significantly lower than in the elevational case, and in practice only  $\hat{\theta}$ -oriented emitters in the vicinity of a silver nanosphere will produce a strong superradiation.

### E. Collective spontaneous emission near a NZE nanoparticle

We will now investigate the effect a metamaterial with dielectric function  $\varepsilon \approx 0$  has on superradiance. These materials have been researched extensively (for example, Refs. [25–27]) and have been shown to display interesting properties, such as very large phase velocity resulting in effective light tunneling through the material. It will be interesting to investigate the effects NZE nanoparticles will have on superradiating sources.

We demonstrate here the effect of a spherical NZE nanoparticle on the superradiance process. Throughout this section, we consider the dielectric function of the NZE to be  $\varepsilon_{\text{NZE}} = -0.01 + 0.01i$ . As in Sec. IV D, we first compare  $\chi(\{\vec{\mathbf{r}}\})$  and  $\gamma$  for several spheres and emitter configurations. These are depicted in Fig. 6.

Contrary to the case of silver spheres, for the radial and azimuthal orientations the NZE sphere significantly inhibits coupling to far-field modes, while significantly enhancing it for the elevational setting, generating radiation intensity of 1400% at an almost 400% rate compared to the free-space case. This can be attributed to the large phase velocity property of the NZE sphere, that in practice makes the emitters optically closer, so that oppositely directed in-phase classical sources would tend to cancel out one another while like-directed ones will radiate in sync. Thus, the situation of a NZE material sphere at the center of a ring of emitters oriented in parallel to the axis of the ring will, in general, enhance their total radiated power, with the optimal radii dictated by classical electromagnetism interference considerations. One may notice a discrepancy between the enhancement of radiated power and the rate enhancement coefficient, most notably for the  $\hat{r}$  and  $\hat{\theta}$  cases; the rates seem to be highest for the sphere radii for which the enhancement is the weakest, especially near the surfaces of the spheres. Since for the NZE the

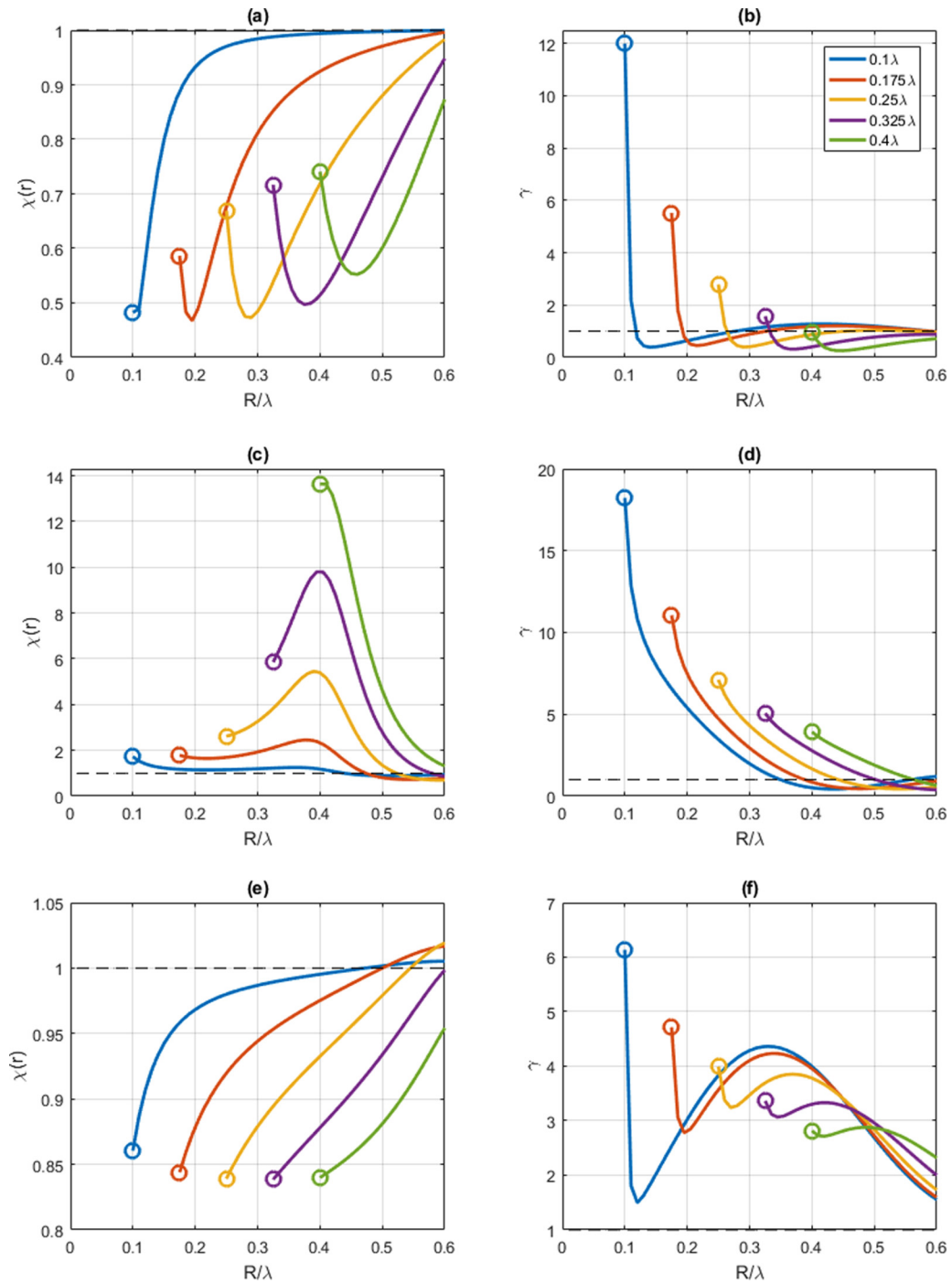


FIG. 6.  $\chi(\{\bar{\mathbf{r}}\})$  and  $\gamma$  for ten identical emitters set equidistantly around the equators of NZE spheres of varying radii (color coded) vs distance from the center of the spheres. (a, c, e)  $\chi(\{\bar{\mathbf{r}}\})$  for radial, elevational, and azimuthal orientations, respectively. (b, d, f)  $\gamma$  for radial, elevational, and azimuthal orientations, respectively.

transmission coefficient for the impinging field is small and the radiation efficiency coefficient is  $\eta_R \rightarrow 1$ , this mismatch cannot be explained by dissipative losses in the sphere. This excess power dissipated from the emitters is stored in near-field modes, not accounted for by  $\eta_R$  or any of the far-field figures of merit defined in Sec. IV A. In Fig. 7 we inspect  $\zeta(\{\bar{\mathbf{r}}\})$  for NZE spheres for the  $\hat{\theta}$  orientation. The two other settings, which are ill-coupled to the far field in free space

(see Fig. 2), are further weakened by the NZE sphere, and we shall therefore not discuss them further.

This figure shows that for all considered sphere radii the dominant radiation mechanism is the emitter-pair interaction with the environment. This further establishes the fact that the NZE sphere enhances the total radiated power of the emitters by bringing them closer optically, as this implies that the emitters couple to the far field through the matter via

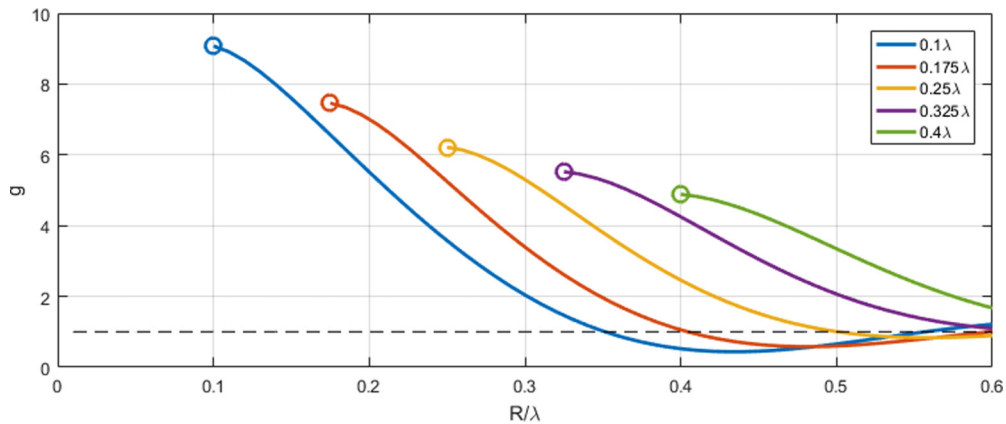


FIG. 7.  $\zeta(\{\mathbf{R}\})$  for ten identical emitters set equidistantly around the equators of NZE spheres of varying radii (color coded) vs distance from the center of the spheres. The emitters are set in elevational orientation.

a collective effect, rather than solely via enlargement of the LDOS separately for each source.

For the NZE sphere case, the introduction of matter enhances the total radiated power of the superradiant process to the far field for the already constructive  $\hat{\theta}$  setting, while weakening it for the already suppressed  $\hat{r}$  and  $\hat{\phi}$  orientations. Note that since  $\eta_R \approx 1$  for all considered distances  $g(\{\mathbf{R}\}) \approx \chi(\{\mathbf{R}\})$  everywhere.

## V. CONCLUSION

We have developed a generalization of Dicke's model of superradiance to include geometric considerations as well as adjacent absorptive material and investigated the effect on the collective spontaneous emission of initially fully excited quantum emitters. This generalization holds for indistinguishable emitters, which impose restriction on the symmetry of the system. Apart from that, the model is valid for any material which may be described by a macroscopic dielectric function, so that one may apply the Huttner-Barnett quantization scheme to it. We have developed a fully quantum-mechanical description of the system, composed of the quantized absorptive material and any number of identical two-level quantum emitters. Two main results emerge from our derivation. The first is the expression for the total radiated power presented in (30), which is separable into a spatial part determined by classical electromagnetism and a temporal part which is quantum mechanical. The second result is the effective rate coefficient of the temporal evolution, given in (24), which stems from two distinct types of emitter-environment interactions—individual emitter environment interactions and emitter-pair environment interactions. This rate coefficient is also determined from electromagnetic boundary conditions.

Examining the results in free space to assess the impact of the emitter geometry on their collective spontaneous emission, we have seen that the emission strength and duration can be elucidated from classical considerations. Orienting the emitters in different directions resulted in differences in emission intensities and durations spanning more than three orders of magnitude, for only ten emitters, a discrepancy that increases with the number of sources. This stresses the impact that source setting has on the collective emission process, a factor

that has mostly been overlooked in previous superradiance works.

We have then investigated the impact of introduction of spherically shaped matter to the system on the superradiant effect, specifically the modification of the characteristic decay rate of the process and the total radiated power. Our model enabled decomposition of the radiated power into contributions from each of the two types of emitter-environment interactions, allowing further insight into the influence of material on the collective process. The analysis of the matter-assisted superradiance focused on spheres of silver and near-zero epsilon material. It was found that silver spheres augment the rate and magnitude of the superradiant pulses for both radial and elevational settings of the emitters, at distances from the surfaces of the spheres with optima predicted from analysis of electromagnetic boundary conditions. However, as silver is highly absorptive for the optical wavelengths considered, a large portion of the power invested in the excitation of the emitters is inevitably coupled to dissipative modes on the sphere rather than to the far field. In the conditions considered, for the radial setting we have calculated a superradiance intensity enhancement factor of about 400% compared to the free-space process, with a rate constant increased by a factor of approximately 1000%. For the elevational setting about 500% intensity enhancement was observed with an approximately 250% rate. The NZE sphere, on the other hand, introduces negligible losses across a sphere much smaller than the optical wavelength inside the material, and due to its optical properties acts to shorten the optical distance between the sources, thus considerably enhancing the coupling to the far field for the elevational orientation by a factor of 14 at almost quadruple rate, but weakening it for the radial and azimuthal cases. Additionally, the rate enhancement coefficient was found to be larger in comparison to the intensity enhancement, therefore indicating power stored in the near-field region.

## ACKNOWLEDGMENT

We would like to acknowledge partial support by the Israeli government program Israeli Centers for Research Excellence (I-CORE): "Circles of Light."

## APPENDIX

We start by considering each TLS being made of charged particles, such that the charge, mass, position operator, and momentum operator of the  $\alpha$ th particle of the  $i$ th emitter are denoted as  $q_{i,\alpha}$ ,  $m_{i,\alpha}$ ,  $\hat{\mathbf{r}}_{i,\alpha}$ , and  $\hat{\mathbf{p}}_{i,\alpha}$ , respectively. The center of the  $i$ th emitter is denoted  $\mathbf{r}_{Q,i}$ . Since the emitters are electrically neutral,

$$\sum_{\alpha} q_{\alpha,i} = 0 \quad (\text{A1})$$

for all  $i$ . We approximate the charge-density operator up to the dipole moment

$$\hat{\rho}_{Q,i}(\mathbf{r}') \approx \sum_{\alpha} q_{i,\alpha} \delta(\mathbf{r}' - \hat{\mathbf{r}}_{i,\alpha}) + \nabla \cdot \left[ \delta(\mathbf{r}' - \hat{\mathbf{r}}_{Q,i}) \sum_{\alpha} (\hat{\mathbf{r}}_{Q,i} - \hat{\mathbf{r}}_{i,\alpha}) q_{i,\alpha} \right] \quad (\text{A2})$$

and define the scalar potential vector for the matter using the longitudinal part of the electric-field operator  $\hat{\mathbf{E}}^{\parallel}(\mathbf{r}, \omega)$  as

$$-\nabla \hat{\phi}_M(\mathbf{r}, \omega) = \hat{\mathbf{E}}^{\parallel}(\mathbf{r}, \omega). \quad (\text{A3})$$

Generalizing the expression obtained in Ref. [28] to the case of  $N$  emitters, the interaction Hamiltonian is

$$\hat{H}_{QF} = - \sum_{i=1}^N \left[ \sum_{\alpha} \frac{q_{i,\alpha}}{m_{i,\alpha}} \hat{\mathbf{p}}_{i,\alpha} \hat{\mathbf{a}}(\mathbf{r}_{i,\alpha}) + \int d^3\mathbf{r} \hat{\rho}_{Q,i}(\mathbf{r}) \hat{\phi}_M(\mathbf{r}) \right], \quad (\text{A4})$$

where

$$\hat{\mathbf{a}}(\mathbf{r}) = \int_0^{\infty} d\omega \hat{\mathbf{a}}(\mathbf{r}, \omega) + \text{H.c.} \quad (\text{A5})$$

is the frequency integral over the vector potential operator, taken to be purely transverse and defined as a function of the effective vacuum operators defined in Sec. II A 1. Therefore, the transverse part of the electric-field operator is defined in the frequency domain to be  $\hat{\mathbf{E}}^{\perp}(\mathbf{r}, \omega) = i\omega \hat{\mathbf{a}}(\mathbf{r}, \omega)$ . The first term of (A4) can be simplified under the dipole approximation to yield

$$- \sum_i \sum_{\alpha} \frac{q_{i,\alpha}}{m_{i,\alpha}} \hat{\mathbf{p}}_{i,\alpha} \hat{\mathbf{a}}(\mathbf{r}_{i,\alpha}) \approx \frac{i}{\hbar} \sum_i [\hat{\mathbf{d}}_{Q,i}, \hat{H}_Q] \hat{\mathbf{a}}(\mathbf{r}_{i,Q}), \quad (\text{A6})$$

where the dipole moment operator of the  $i$ th emitter is introduced in the coordinate system of the  $i$ th dipole:

$$\hat{\mathbf{d}}_{Q,i} = \sum_{\alpha} q_{i,\alpha} \hat{\mathbf{r}}_{i,\alpha}. \quad (\text{A7})$$

This operator operates on states of the  $i$ th emitter, such that

$$\begin{aligned} \langle e | \hat{\mathbf{d}}_{Q,i} | g \rangle_i &= \langle g | \hat{\mathbf{d}}_{Q,i} | e \rangle_i \equiv \mathbf{d}_i, \\ \langle e | \hat{\mathbf{d}}_{Q,i} | e \rangle_i &= \langle g | \hat{\mathbf{d}}_{Q,i} | g \rangle_i = 0, \end{aligned} \quad (\text{A8})$$

so that eventually one arrives at

$$\frac{i}{\hbar} \sum_i [\hat{\mathbf{d}}_{Q,i}, \hat{H}_Q] \hat{\mathbf{a}}(\mathbf{r}_{i,Q}) = i\omega_Q \sum_i (\hat{\sigma}_i^{\dagger} - \hat{\sigma}_i) \mathbf{d}_i \hat{\mathbf{a}}(\mathbf{r}_{i,Q}). \quad (\text{A9})$$

We define the vector field operator

$$\hat{\mathcal{E}}(\mathbf{r}) = \hat{\mathcal{E}}^{(+)}(\mathbf{r}) + \hat{\mathcal{E}}^{(-)}(\mathbf{r}), \quad (\text{A10})$$

where

$$\hat{\mathcal{E}}^{(+)}(\mathbf{r}) = \int_0^{\infty} d\omega \hat{\mathbf{E}}(\mathbf{r}, \omega). \quad (\text{A11})$$

Under the assumption that the electric field is approximately monochromatic with frequency  $\omega_Q$ , and under employment of the RWA, from the definition of the transverse part of the electric-field operator [see (A10)] we obtain

$$\begin{aligned} & - \sum_i \sum_{\alpha} \frac{q_{i,\alpha}}{m_{i,\alpha}} \hat{\mathbf{p}}_{i,\alpha} \hat{\mathbf{a}}(\mathbf{r}_{i,\alpha}) \\ & \approx - \sum_i \mathbf{d}_i [\sigma_i^{\dagger} \hat{\mathcal{E}}^{\perp(+)}(\mathbf{r}_{Q,i}) + \sigma_i \hat{\mathcal{E}}^{\perp(-)}(\mathbf{r}_{Q,i})]. \end{aligned} \quad (\text{A12})$$

For the second term in (A4), substitution of (A2) and (A3) and application of the RWA produces

$$\begin{aligned} & - \sum_{i=1}^N \int d^3\mathbf{r} \hat{\rho}_{Q,i}(\mathbf{r}) \hat{\phi}_M(\mathbf{r}) \\ & \approx - \sum_{i=1}^N \mathbf{d}_i \{ \sigma_i^{\dagger} \hat{\mathcal{E}}^{\parallel(+)}(\mathbf{r}_{Q,i}) + \sigma_i \hat{\mathcal{E}}^{\parallel(-)}(\mathbf{r}_{Q,i}) \} \end{aligned} \quad (\text{A13})$$

so that the interaction Hamiltonian is simply

$$\hat{H}_{QF} = - \sum_{i=1}^N \mathbf{d}_i \{ \sigma_i^{\dagger} \hat{\mathcal{E}}^{(+)}(\mathbf{r}_{Q,i}) + \sigma_i \hat{\mathcal{E}}^{(-)}(\mathbf{r}_{Q,i}) \}. \quad (\text{A14})$$

- [1] J. B. Khurgin and A. Boltasseva, Reflecting upon the losses in plasmonics and metamaterials, *MRS Bulletin* **37**, 768 (2012).
- [2] E. M. Purcell, Spontaneous emission probabilities at radio frequencies, *Confined Electrons and Photons* (Springer, New York, 1995).
- [3] J. Zhang, M. Wubs, P. Ginzburg, G. Wurtz, and A. V. Zayats, Transformation quantum optics: Designing spontaneous

- emission using coordinate transformations, *J. Opt.* **18**, 044029 (2016).
- [4] A. N. Poddubny, P. Ginzburg, P. A. Belov, A. V. Zayats and Y. S. Kivshar, Tailoring and enhancing spontaneous two-photon emission using resonant plasmonic nanostructures, *Phys. Rev. A* **86**, 033826 (2012).
- [5] R. H. Dicke, Coherence in spontaneous radiation processes, *Phys. Rev.* **93**, 99 (1954).

- [6] V. N. Pustovit and T. V. Shahbazyan, Plasmon-mediated superradiance near metal nanostructures, *Phys. Rev. B* **82**, 075429 (2010).
- [7] L. Allen and J. H. Eberly, *Optical Resonance and Two-Level Atoms* (Wiley, New York, 1975).
- [8] M. Gross and S. Haroche, Superradiance: An essay on the theory of collective spontaneous emission, *Phys. Rep.* **93**, 301 (1982).
- [9] G. S. Agarwal, Quantum statistical theories of spontaneous emission and their relation to other approaches, *Quantum Optics* (Springer, Berlin, 1974).
- [10] R. Bonifacio, P. Schwendimann, and F. Haake, Quantum statistical theory of superradiance I, *Phys. Rev. A* **4**, 302 (1971).
- [11] B. Huttner and S. M. Barnett, Quantization of the electromagnetic field in dielectrics, *Phys. Rev. A* **46**, 4306 (1992).
- [12] L. Knöll, S. Scheel, and D. G. Welsch, QED in dispersing and absorbing media, [arXiv:quant-ph/0006121](https://arxiv.org/abs/quant-ph/0006121).
- [13] T. Gruner and D. G. Welsch, Green-function approach to the radiation-field quantization for homogeneous and inhomogeneous Kramers-Kronig dielectrics, *Phys. Rev. A* **53**, 1818 (1996).
- [14] H. T. Dung, L. Knöll, and D. G. Welsch, Resonant dipole-dipole interaction in the presence of dispersing and absorbing surroundings, *Phys. Rev. A* **66**, 063810 (2002).
- [15] E. Schmidt, J. Jeffers, S. M. Barnett, L. Knöll, and D. G. Welsch, Quantum theory of light in nonlinear media with dispersion and absorption, *J. Mod. Opt.* **45**, 377 (1998).
- [16] T. Gruner and D. G. Welsch, Correlation of radiation-field ground-state fluctuations in a dispersive and lossy dielectric, *Phys. Rev. A* **51**, 3246 (1995).
- [17] L. Novotny and B. Hecht, *Principles of Nano-Optics* (Cambridge University, Cambridge, England, 2012).
- [18] G. Schlegel, J. Bohnenberger, I. Potapova, and A. Mews, Fluorescence Decay Time of Single Semiconductor Nanocrystals, *Phys. Rev. Lett.* **88**, 137401 (2002).
- [19] U. Resch-Genger, M. Grabolle, S. Cavaliere-Jaricot, R. Nitschke, and T. Nann, Quantum dots versus organic dyes as fluorescent labels, *Nat. Methods* **5**, 763 (2008).
- [20] F. T. Arecchi and D. M. Kim, Line shifts in cooperative spontaneous emission, *Opt. Commun.* **2**, 324 (1970).
- [21] R. Friedberg and S. R. Hartmann, Temporal evolution of superradiance in a small sphere, *Phys. Rev. A* **10**, 1728 (1974).
- [22] R. Ruppin, Decay of an excited molecule near a small metal sphere, *J. Chem. Phys.* **76**, 1681 (1982).
- [23] A. P. Moneda and D. P. Chrissoulidis, Dyadic Green's function of a sphere with an eccentric spherical inclusion, *JOSA A* **24**, 1695 (2007).
- [24] H. U. Yang, J. D'Archangel, M. L. Sundheimer, E. Tucker, G. D. Boreman, and M. B. Raschke, Optical dielectric function of silver, *Phys. Rev. B* **91**, 235137 (2015).
- [25] A. Alù, M. G. Silveirinha, A. Salandrino, and N. Engheta, Epsilon-near-zero metamaterials and electromagnetic sources: Tailoring the radiation phase pattern, *Phys. Rev. B* **75**, 155410 (2007).
- [26] R. J. Pollard, A. Murphy, W. R. Hendren, P. R. Evans, R. Atkinson, G. A. Wurtz, A. V. Zayats, and V. A. Podolskiy, Optical Nonlocalities and Additional Waves in Epsilon-Near-Zero Metamaterials, *Phys. Rev. Lett.* **102**, 127405 (2009).
- [27] M. Silveirinha and N. Engheta, Tunneling of Electromagnetic Energy through Subwavelength Channels and Bends using  $\epsilon$ -Near-Zero Materials, *Phys. Rev. Lett.* **97**, 157403 (2006).
- [28] H. T. Dung, L. Knöll, and D. G. Welsch, Spontaneous decay in the presence of dispersing and absorbing bodies: General theory and application to a spherical cavity, *Phys. Rev. A* **62**, 053804 (2000).